AJNR

MR of the cerebral operculum: topographic identification and measurement of interopercular distances in healthy infants and children.

C Y Chen, R A Zimmerman, S Faro, B Parrish, Z Wang, L T Bilaniuk and T Y Chou

AJNR Am J Neuroradiol 1995, 16 (8) 1677-1687
http://www.ajnr.org/content/16/8/1677

MR of the Cerebral Operculum: Topographic Identification and Measurement of Interopercular Distances in Healthy Infants and Children

Cheng-Yu Chen, Robert A. Zimmerman, Scott Faro, Beth Parrish, Zhiyue Wang, Larissa T. Bilaniuk, and Ting-Ywan Chou

PURPOSE: To evaluate the role of axial, coronal, and sagittal MR in identification of surface landmarks of the cerebral operculum and to determine the reference values of interopercular distances of each hemisphere in healthy infants and children on MR images. **METHODS:** Two hundred fourteen cerebral opercula of 35 healthy infants and 72 healthy children were retrospectively evaluated from 107 routine MR brain examinations. The surface landmarks of the operculum and interopercular distances of each hemisphere, which were subjectively divided into anterior interopercular distance (anterior sylvian width) and posterior interopercular distance (posterior sylvian width), were recorded from axial, coronal, and sagittal MR images, respectively. The mean value of anterior interopercular distance of each hemisphere was obtained by averaging two linear measurements of the anterior sylvian width from lateral, sagittal, and axial planes of the same side. Likewise, the posterior interopercular distance of each side of the brain was obtained from averaging of two measurements on lateral, sagittal, and coronal planes. **RESULTS:** The landmarks of the operculum were best identified by sagittal MR, followed by axial and coronal images. The average values of left anterior interopercular distance, right anterior interopercular distance, left posterior interopercular distance, and right posterior interopercular distance in infants were 1.9 ± 1.3, 1.6 ± 1.1, 0.4 ± 0.7, and 0.2 ± 0.4 mm, and in children, 0.9 ± 1.3, 1.0 ± 1.4, 0.03 ± 0.23, and 0.01 ± 0.07 mm, respectively. Infants showed significantly wider interopercular distances than children. Left anterior interopercular distance was significantly wider than right in infants, but not in children. Male children displayed a more significant increase in anterior interopercular distance than did female children. There was no statistic difference in measurements of anterior interopercular distance and posterior interopercular distance between female and male infants. **CONCLUSIONS:** The operculum should be evaluated with MR in three planes. Infants may show conspicuous sylvian fissures that should not exceed 4.5 mm (mean + 2 SD) anteriorly on axial and sagittal planes and 1.8 mm posteriorly on sagittal and coronal planes. Healthy children who have fully developed opercula should have an anterior interopercular distance of no more than 3.5 mm and a posterior interopercular distance of 0.5 mm.

Index terms: Brain, anatomy; Brain, measurements; Magnetic resonance, in infants and children

AJNR Am J Neuroradiol 16:1677–1687, September 1995

Received July 15, 1994; accepted after revision March 27, 1995.

From the Department of Radiology, The Children's Hospital of Philadelphia (Pa) (C.-Y.C., R.A.Z., S.F., Z.W., L.T.B.); the Department of Radiology, Tri-Service General Hospital, National Defense Medical Center, Taiwan, Republic of China (C.-Y.C., T.-Y.C.); and the Division of Child Development and Rehabilitation, Children's Seashore House and Children's Hospital of Philadelphia (Pa) (B.P.).

Address reprint requests to Robert A. Zimmerman, MD, Department of Radiology, The Children's Hospital of Philadelphia, 34th Street and Civic Center Boulevard, Philadelphia, PA 19104.

AJNR 16:1677–1687, Sep 1995 0195-6108/95/1608–1677

The *cerebral operculum* refers to portions of the frontal, parietal, and temporal lobes adjacent to the sylvian fissure and overlying the insula (1, 2). These parts of the cortex, which include the posterior inferior frontal gyrus, the inferior precentral and postcentral gyri, the supramarginal gyrus, the angular gyrus, and the superior temporal gyrus, have fairly consistent landmarks that have been studied, mostly at the inferior precentral region, in the adult brain with sagittal magnetic resonance (MR) images (3–5). The development of the opercula (the

''opercularization''), which is seen as an expression of the functional maturity of the brain (6), also can be evaluated by MR. Tatum et al measured the separation from frontal to temporal tip on axial MR imaging in 125 pediatric patients and concluded that a separation more than 3 mm is abnormal, implicating a developmental arrest of the operculum (7). In this MR study, we focus on the normal opercular anatomy in infants and children, because the operculum encompasses areas vital for both the perception of spoken language and motor aspects of speech (areas 44 and 45 and posterior part of 22 and 39 on Brodmann's chart of cortical areas) (1, 8). Identification of the operculum as underdeveloped or abnormal may have implications for the educational treatment of children with developmental delays, particularly in speech and language.

The purpose of this study is to compare the capabilities and limitations of axial, coronal, and sagittal MR planes in location of the opercular anatomy and to determine the normal separation between (*a*) the frontal and temporal opercula (the anterior interopercular distance or the width of the anterior portion of the sylvian fissure), and (*b*) the parietal and temporal opercula (the posterior interopercular distances or the width of the posterior portion of the sylvian fissure) on axial, sagittal, and coronal MR in healthy infants (younger than 1 year of age) and children (older than 1 year of age).

Methods

Subjects

This study was retrospectively undertaken in 35 infants (16 boys and 19 girls), ranging in age from birth to 1 year, and 72 children (45 boys and 27 girls), ranging in age from more than 1 year to 16 years, from two institutes during a period of 3 years (1990 through 1992). Subjects were categorized into "infants" and "children" according to the cerebral gyration stage of Martin et al, which states that the adult gyration pattern is usually achieved after 1 year of age (9). Subjects who were included had normal findings on laboratory and initial MR examination and had no clinical evidence of developmental delays. They were primarily referred for temporary neurologic dysfunction including seizure (n = 63), spasmus nutans (n = 6), infantile spasm (n = 5), head injury (n = 11), migraine (n = 2), microcephaly (n = 7), macrocephaly (n = 8), apnea (n = 2), ticks (n = 1), small stature (n = 1), and precocious puberty (n = 1). All the MR images were verified as normal after careful review by two neuroradiologists. Twenty-one patients who were initially enrolled in this study were excluded because of suspicious brain atrophy or external hydrocephalus after the review procedure.

Imaging Technique

The MR images of the 107 subjects were obtained with two 1.5-T units (Siemens SP, Germany; Picker Vista HPQ, United States). The imaging sequences consisted of spin-echo, T1-weighted, 500-600/15-40/1-2 (repetition time/echo time/excitations) axial and sagittal images with 3- to 5-mm section thickness and T2-weighted, 2800-3000/90-120/1-2 axial and coronal images with 5-mm section thickness. Additional coronal T1-weighted images were obtained occasionally for further information. Subjects with seizure were examined with standard seizure protocol including coronal T1-weighted and T2-weighted scans perpendicular to the hippocampus to rule out the possibility of mesial temporal sclerosis or atrophy. The matrix size was 256 $\times$ 256 in the sagittal plane and 160-192 $\times$ 256 in the axial or coronal planes. The field of view was variable from 20 to 25 cm, depending on the head size of the patient.

Topographic Identification

The identification of the major surface landmarks of the operculum (Fig 1) by lateral sagittal T1-weighted images, axial T1- or T2-weighted images, and coronal T2-weighted images were recorded to compare the ability of these MR planes to show the opercular anatomy. Because the variation of the inferior precentral sulcus and anterior ascending sylvian rami was small according to Ebeling et al (3), we did not include this variation in the analysis. The methods used to identify the perisylvian anatomy on sagittal images have been described elsewhere (3, 5) (Fig 2A and B). On axial planes, two techniques were applied in each case for the identification of the opercular surface landmarks:

1. The anterior ascending ramus of the sylvian fissure is continuous with the circular (periinsular) sulcus (2, 10), which can be easily identified by tracing the anterior portion of the sylvian fissure cephalad (Figs 3A and B). The inferior precentral sulcus runs parallel and next to the anterior ascending ramus of the sylvian fissure. The pars opercularis (area 44 on Brodmann's chart of cortical areas) lies between these two sulci in the dominant hemisphere. The inferior central and postcentral sulci are the next two sulci posterior to the precentral sulci.
2. The inferior precentral and central sulci also can be identified by tracing caudally from the high convexity of the hemisphere. The location method for these sulci at the high convexity has been described by Kido et al (11). The identification of the supramarginal and angular gyri can be made by identifying the

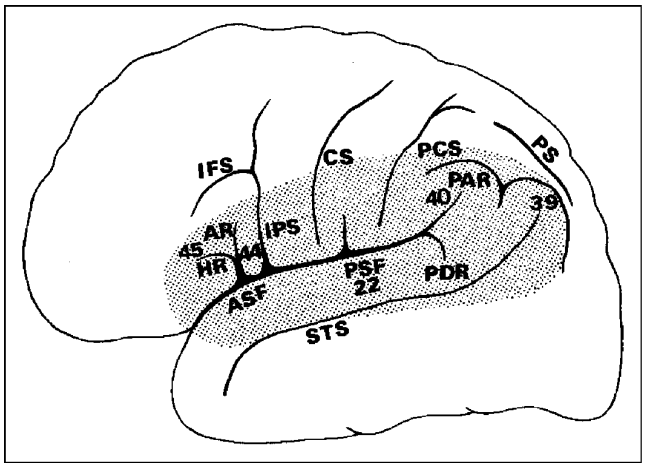

Fig 1. Major surface landmarks of the operculum (*stippled area*) on lateral view of cerebral hemisphere. (See key for abbreviations.)

Key to Abbreviations in Figures and Tables

AG indicates angular gyrus; AR, anterior ascending ramus of sylvian fissure; ASF, anterior sylvian fissure; CIS, circular sulcus; CS, central sulcus; HR, anterior horizontal ramus of sylvian fissure; IFS, inferior frontal sulcus; IPS, inferior precentral sulcus; PS, interparietal sulcus; IS, insular sulcus; PAR, posterior ascending ramus of sylvian fissure; PCS, postcentral sulcus; PDR, posterior descending ramus of sylvian fissure; POP, pars opercularis; POR, pars orbicularis; PSF, posterior sylvian fissure; PT, pars triangularis; SMG, supramarginal gyrus; STS, superior temporal sulcus; 44, area 44 on Brodmann chart, same as POP; 45, area 45 on Brodmann chart, same as POR; 22, area 22 on Brodmann chart; 39, area 39 on Brodmann chart, same as AG; and 40, area 40 on Brodmann chart, same as SMG.

postcentral and the interparietal sulcus. The supramarginal gyrus is located at the posterior parietal region posterior to the postcentral sulcus. The angular gyrus lies lateral to the interparietal sulcus and posterior to the supramarginal gyrus at the posterior parietal region. The posterior end of the superior temporal sulcus, which is draped over by the angular gyrus, can be located lateral to the posterior interparietal sulcus (Figs 3C and D).

The landmarks used for identification of the opercular surface anatomy on coronal images are inferior frontal sulcus, horizontal sylvian fissure, and the superior temporal sulcus, which run perpendicular to the section plane (Fig 4A). The posterior inferior frontal gyrus (Broca's area on the dominant hemisphere) and the inferior precentral gyrus can be identified by tracing the inferior frontal sulcus back to the junction where the inferior frontal sulcus joins the precentral sulcus. Moreover, the inferior precentral gyrus itself has a characteristic "hook" appearance making the identification easy (Fig 4B). The supramarginal and angular gyri are located at the ends of the sylvian fissure and superior temporal sulcus, respectively (Figs 4C and D). The pars orbicularis (lateral part of orbital gyrus that borders the inferior frontal gyrus) is at the posterolateral portion of the frontal lobe within the anterior cranial fossa.

Films were interpreted by one neuroradiologist who had knowledge of these identification methods before reading. Additional neuroradiologists joined in the interpretation when the images were equivocal. The intraobserver variability was tested in these cases and was shown to be negligible.

Measurements of Interopercular Distances

The anterior interopercular distance (anterior sylvian width) was defined as the distance between the posteroinferior border of the inferior frontal gyrus and the superoanterior border of the temporal lobe, which was shown as *a* in

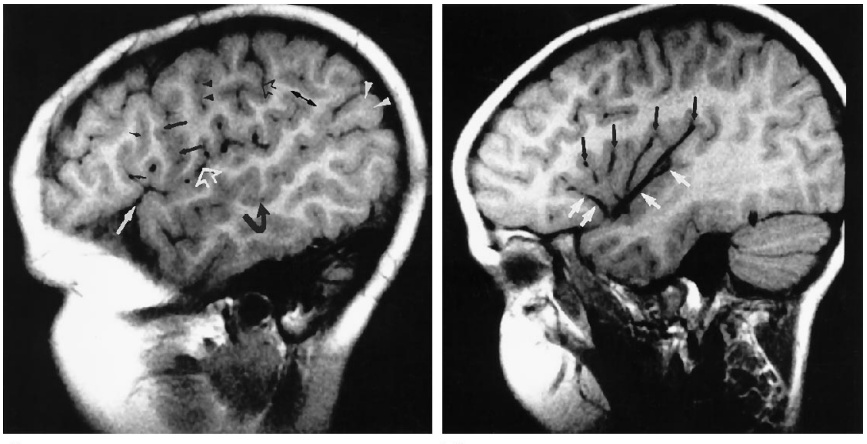

Fig 2. Lateral sagittal T1-weighted images (600/20/1) in a 7-year-old boy.

A, The AR (*short black arrows*), IPS (*black arrows*), CS (*arrowheads*), PCS (*small black open arrow*), ASF (*white arrow*), PSF (*larger white open arrow*), STS (*black curved arrows*), area 40 (*doubled arrow*), and area 39 (*white arrowheads*) are shown. Broca's area is located between the AR and the IPS on the dominant hemisphere.

B, Eight millimeters medial to A, the insular sulci (*black arrows*) are oriented vertically on which the insular segment of middle cerebral artery traverses. The anterior and posterior portions of the circular sulcus are indicated by *white arrowheads*. (See key for abbreviations.)

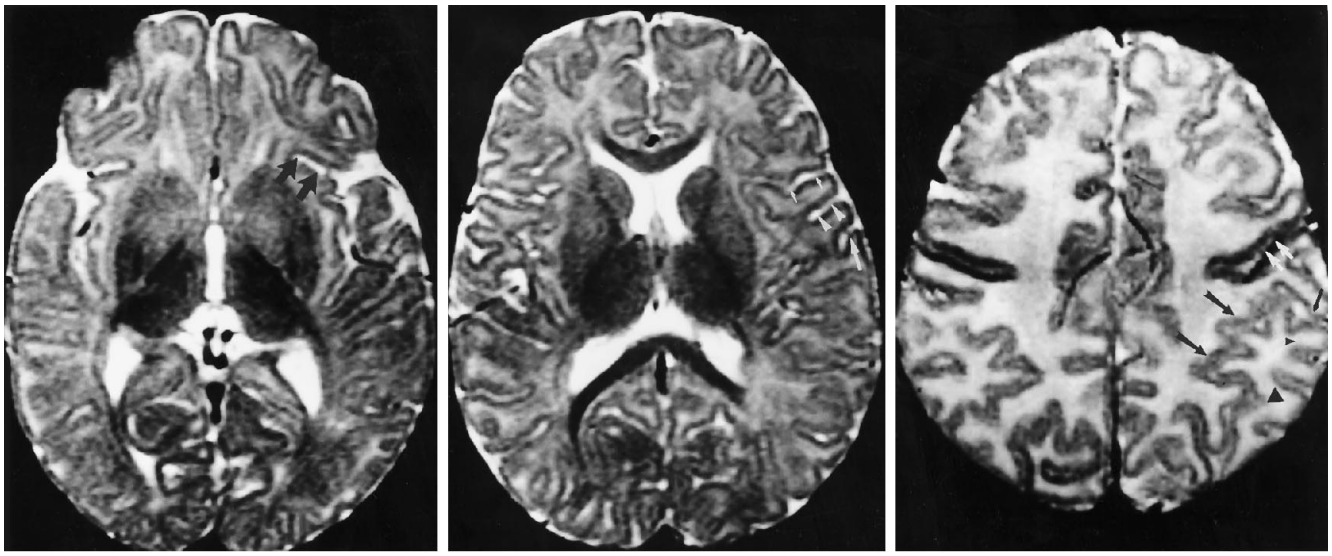

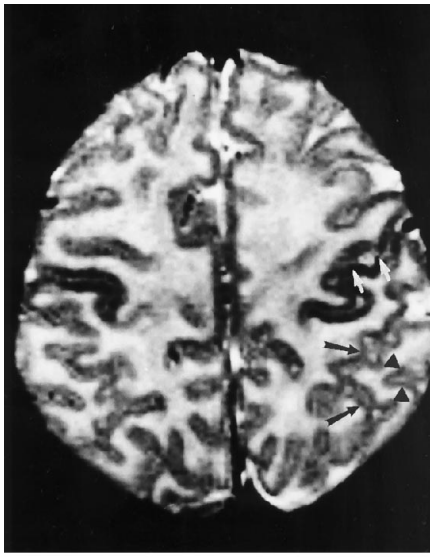

Fig 3. *A*, Axial T2-weighted (3000/120/1) images at thalamus level in a 7-month-old child showed the anterior portion of CIS (*black arrows*).

B, Contiguous section 5 mm cephalad to A reveals the parietal opercula and their surface landmarks: AR (*small white arrows*), IPS (*white arrowheads*), CS (*white arrows*).

C and *D*, Contiguous axial T2-weighted (3000/120/1) images at parietal convexity in a neonate. The CS (*small white arrows*) can be easily identified by recognizing the myelinated pericentral gyri. The SMG (*small arrowheads*) is located posterior to the PCS (*small black arrow*) and lateral to the PS (*black arrows*). AG (*arrowheads*) is the gyrus posterior to the CS and lateral to the PS. (See key for abbreviations.)

the sagittal plane and *c* in the axial plane at the level of the hypothalamus as illustrated in Figure 5. The posterior interopercular distance (posterior sylvian width) was the separation between the inferior border of the parietal operculum (the inferior pericentric gyri) and the superior border of the temporal operculum (the superior temporal gyrus), which was shown as *b* in the sagittal plane and as *d* in the coronal plane, 5 mm posterior to the M-1 segments of middle cerebral arteries. The linear measurements of a and b were made on sagittal T1-weighted image, 10 to 12 mm from the inner table where the interopercular relationship could be recognized. The distances c and d were obtained by measuring on axial T1-weighted and on coronal T2-weighted images, respectively. The mean anterior interopercular distance of each hemisphere was an averaging value from a and c. Similarly, the mean posterior interopercular distance of each hemisphere was made by averaging of b and d.

The measurements were made by one of the authors (C.C.) using a hand-held electronic caliper, which was submillimeter in accuracy. Each measurement was obtained directly from the image and then was calculated from the 5- or 10-cm scale on the same film to get the true distance. The reference scales (5 or 10 cm) on each film had been corrected beforehand by the same caliper. The measurement difference between those obtained by the hand-held caliper and computer software in the MR console was insignificant in 20 patients. Interobserver and intraobserver variability was evaluated in the first 25 patients and was shown to be negligible. Subjects were categorized into two groups: infants (age less than 1 year) and children (age more than 1 year).

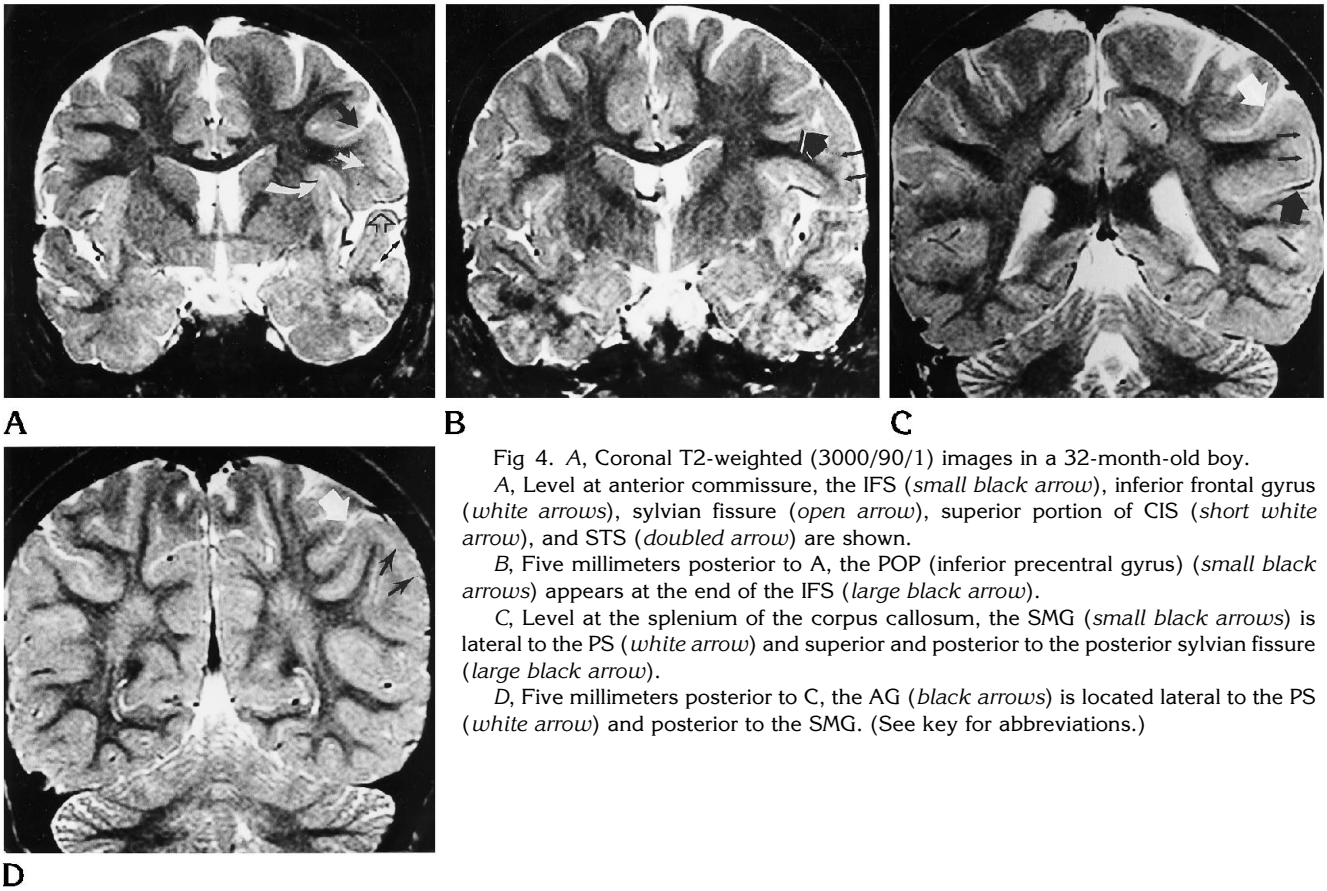

Fig 4. *A*, Coronal T2-weighted (3000/90/1) images in a 32-month-old boy.

A, Level at anterior commissure, the IFS (*small black arrow*), inferior frontal gyrus (*white arrows*), sylvian fissure (*open arrow*), superior portion of CIS (*short white arrow*), and STS (*doubled arrow*) are shown.

B, Five millimeters posterior to A, the POP (inferior precentral gyrus) (*small black arrows*) appears at the end of the IFS (*large black arrow*).

C, Level at the splenium of the corpus callosum, the SMG (*small black arrows*) is lateral to the PS (*white arrow*) and superior and posterior to the posterior sylvian fissure (*large black arrow*).

D, Five millimeters posterior to C, the AG (*black arrows*) is located lateral to the PS (*white arrow*) and posterior to the SMG. (See key for abbreviations.)

Statistical Analysis

Calculations of average values were made for each item in both the infant and children groups, as well as their standard deviations. The Student's *t* test for unpaired samples then was calculated to determine whether significant differences were present between the infants and children for each item. Determination of significant differences between girls and boys and left hemisphere and right hemisphere (Student's *t* test) in each group was performed.

Results

Topographic Information

Most major surface landmarks of the operculum were identified by sagittal T1-weighted images (Figs 4A and B). Axial T1- or T2-weighted MR images were able to delineate the major gyri in the frontal, parietal, and temporal opercula, but could not show the posterior sylvian fissure

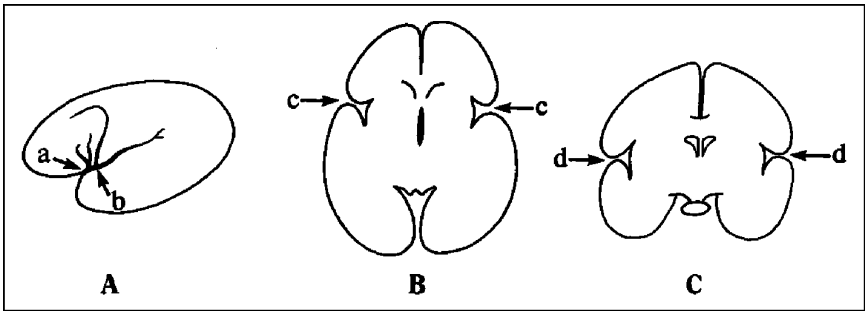

Fig 5. Schematic illustration of anterior interopercular distances (*a* and *c*) and posterior interopercular distances (*b and d*) on sagittal (*A*), axial (*B*), and coronal (*C*) planes.

TABLE 1: Frequency of topographic identification of opercular surface landmarks with sagittal, axial, and coronal MR in 214 hemispheres

	Sagittal (n = 214)	Axial (n = 214)	Coronal (n = 214)
AG	191 (89.3%)	198 (92.5%)	161 (75.2%)
AR	212 (99.1%)	202 (94.4%)	0 (0%)
ASF	214 (100%)	214 (100%)	214 (100%)
CIS	214 (100%)	214 (100%)	214 (100%)
CS	212 (99.1%)	202 (94.4%)	0 (0%)
HR	200 (93.5%)	164 (76.7%)	0 (0%)
IFS	207 (96.7%)	0 (0%)	195 (91%)
IPCS	212 (99.1%)	202 (94.4%)	0 (0%)
IPS	139 (65%)	198 (92.7%)	161 (75.2%)
IS	214 (100%)	214 (100%)	0 (0%)
PAR	205 (95.8%)	0 (0%)	113 (52.8%)
PDR	117 (54.7%)	0 (0%)	0 (0%)
POP	212 (99.1%)	202 (94.4%)	194 (90.7%)
POR	214 (100%)	214 (100%)	214 (100%)
PSF	214 (100%)	163 (76%)	214 (100%)
PT	212 (99.1%)	202 (94.4%)	0 (0%)
SMG	214 (100%)	198 (92.5%)	214 (100%)
STS	214 (100%)	0 (0%)	214 (100%)

Note.—See key for abbreviations.

and sulci, which run parallel or near parallel to the scanning plane. Coronal T2-weighted imaging could demonstrate 100% of the anterior and posterior sylvian fissure, as well as the superior temporal sulci, but not the inferior precentral sulci and ascending sylvian rami, which were important landmarks to identify Broca's area. The overall frequency of identification of each landmark by axial, coronal, and sagittal MR imaging are summarized in Table 1.

Measurements of Interopercular Distances

Table 2 shows the average values of each interopercular distance for the mean anterior interopercular distance and mean posterior interopercular distance in infants and children. Infants showed significantly wider anterior interopercular distance (left, 1.9 ± 1.3 mm; right, 1.6 ± 1.1 mm) and posterior interopercular distance (left, 0.4 ± 0.7 mm; right, 0.2 ± 0.4 mm)

TABLE 2: Average values of interopercular distances in infants (group 1) compared with children (group 2)

	Group 1 (age <1 yr, n = 35)	Group 2 (age >1 yr, n = 72)	Significance
a*(L)	2.1 ± 1.5	0.9 ± 1.5	$P < 0.001$
b†(L)	0.5 ± 0.7	0.03 ± 0.24	$P = 0.01$
c‡(L)	1.8 ± 1.3	0.8 ± 1.3	$P < 0.001$
d§(L)	0.4 ± 0.7	0.04 ± 0.24	$P = 0.007$
a*(R)	1.8 ± 1.3	1.1 ± 1.7	$P = 0.04$
b†(R)	0.2 ± 0.4	0.02 ± 0.14	$P = 0.016$
c‡(R)	1.5 ± 1.1	0.9 ± 1.4	$P = 0.11$
d§(R)	0.2 ± 0.5	0	‖
MAIO¶(L)	1.9 ± 1.3	0.9 ± 1.3	$P < 0.001$
MAIO¶(R)	1.6 ± 1.1	1.0 ± 1.4	$P = 0.014$
MPIO#(L)	0.4 ± 0.7	0.03 ± 0.23	$P = 0.002$
MPIO#(R)	0.2 ± 0.4	0.01 ± 0.07	$P = 0.007$

*Anterior interopercular distance measured on lateral sagittal MR images.
† Posterior interopercular distance measured on lateral sagittal MR images.
‡ Anterior interopercular distance measured on axial MR images.
§ Posterior interopercular distance measured on coronal images.
‖ No variance in group 2 for independent sample *t* test.
¶ Mean anterior interopercular distance =(a + b)/2].
# Mean posterior interopercular distance =(c + d)/2.

TABLE 3: Average values of left and right interopercular distance and their comparison in two age groups

	Group 1 (age <1 year, n = 35)			Group 2 (age >1 year, n = 72)		
	Left	Right	Significance	Left	Right	Significance
a*	2.1 ± 1.5	1.8 ± 1.3	$P = 0.094$	0.9 ± 1.5	1.1 ± 1.7	$P = 0.125$
b†	0.5 ± 0.7	0.2 ± 0.4	$P = 0.045$	0.03 ± 0.24	0.02 ± 0.14	$P = 0.734$
c‡	1.8 ± 1.3	1.5 ± 1.1	$P = 0.036$	0.8 ± 1.3	0.9 ± 1.4	$P = 0.488$
d§	0.4 ± 0.7	0.2 ± 0.5	$P = 0.193$	0.04 ± 0.24	0	$P = 0.176$
MAIO‖	1.9 ± 1.3	1.6 ± 1.1	$P = 0.048$	0.86 ± 1.31	1.01 ± 1.43	$P = 0.214$
MPIO¶	0.4 ± 0.7	0.2 ± 0.4	$P = 0.073$	0.03 ± 0.23	0.01 ± 0.07	$P = 0.385$

*Anterior interopercular distance measured on lateral sagittal MR images.
† Posterior interopercular distance measured on lateral sagittal MR images.
‡ Anterior interopercular distance measured on axial MR images.
§ Posterior interopercular distance measured on coronal MR images.
‖ Mean anterior interopercular distance.
¶ Mean posterior interopercular distance.

than children ($P < .05$). Table 3 shows the difference between the left and the right interopercular distances. Left anterior interopercular distance was significantly wider than the right in infants ($P < .05$). In children, there was no difference between the left and the right interopercular distances. Similar comparison between gender shows a significant increase in the anterior interopercular distance in male children when compared with female children (Table 4). There was no statistical difference in measurements of anterior interopercular distance and posterior interopercular distance between male and female infants.

Linear measurements of mean anterior interopercular distance and mean posterior interopercular distance as a function of age are shown in Figure 6. Linear regression analysis revealed significant decrease in interopercular distances as a function of age from birth to 16 years. Mean posterior interopercular distance was small at birth and gradually decreased toward 0. Mean anterior interopercular distance could be as large as 4.5 mm (mean + 2 SD) at birth but decreased to 0 as the age increased.

Discussion

The cerebral operculum comprises parts of the frontal, temporal, and parietal lobes that override the insula (the central lobe or island of Reil) and appose one another to form the lateral sulcus (the sylvian fissure). These parts of the

TABLE 4: Average values of interopercular distances of male and female subjects in two age groups

	Group 1 (age <1 year)			Group 2 (age >1 year)		
	Male (n = 16)	Female (n = 19)	Significance	Male (n = 45)	Female (n = 27)	Significance
a*(L)	1.95 ± 0.96	2.2 ± 0.96	$P = 0.661$	1.3 ± 1.5	0.4 ± 1.2	$P = 0.011$
b† (L)	0.5 ± 0.6	0.5 ± 0.8	$P = 0.998$	0.04 ± 0.30	0	‖
c‡ (L)	1.94 ± 0.99	1.72 ± 1.52	$P = 0.598$	1.13 ± 1.46	0.20 ± 0.72	$P = 0.001$
d§ (L)	0.45 ± 0.60	0.33 ± 0.79	$P = 0.619$	0.06 ± 0.30	0	‖
a* (R)	1.93 ± 0.96	1.64 ± 1.61	$P = 0.518$	1.46 ± 1.70	0.62 ± 1.44	$P = 0.03$
b† (R)	0.2 ± 0.4	0.2 ± 0.4	$P = 0.972$	0	0.04 ± 0.23	‖
c‡ (R)	1.86 ± 0.96	1.23 ± 1.17	$P = 0.089$	1.09 ± 1.46	0.52 ± 1.15	$P = 0.07$
d§ (R)	0.13 ± 0.36	0.25 ± 0.52	$P = 0.446$	0	0	‖
MAIO¶ (L)	1.95 ± 0.94	1.94 ± 1.51	$P = 0.985$	1.20 ± 1.39	0.30 ± 0.94	$P = 0.002$
MAIO¶ (R)	1.89 ± 0.94	1.43 ± 1.22	$P = 0.217$	1.27 ± 1.47	0.57 ± 1.26	$P = 0.036$
MPIO# (L)	0.456 ± 0.589	0.397 ± 0.779	$P = 0.801$	0.05 ± 0.24	0	‖
MPIO# (R)	0.17 ± 0.37	0.23 ± 0.42	$P = 0.652$	0	0.02 ± 0.12	‖

*Anterior interopercular distance measured on lateral sagittal MR images.
† Posterior interopercular distance measured on lateral sagittal MR images.
‡ Anterior interopercular distance measured on axial MR images. § Posterior interopercular distance measured on coronal MR images.
‖ No variance in group 2 for independent sample t test.
¶ Mean anterior interopercular distance = (a+b)/2.
# Mean posterior interopercular distance = (c+d)/2.

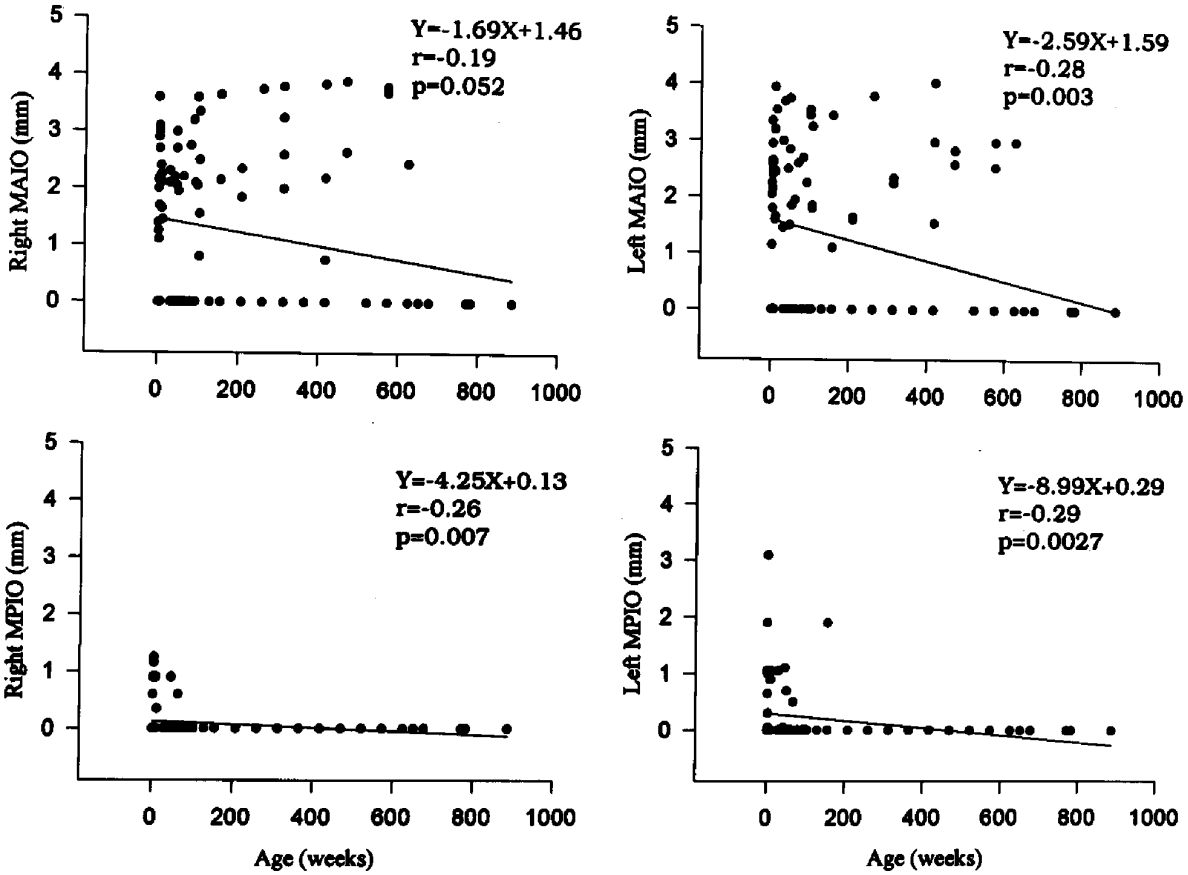

Fig 6. Linear regression analysis curves of mean anterior interopercular distance (*MAIO, above*) and mean posterior interopercular distance (*MPIO, below*) as function of age from birth to 16 years. Significant decrease in both anterior and posterior interopercular distances with increasing age is shown.

cortices encompass areas important for auditory function (areas 41 and 42 on Brodmann's chart), secondary somatic sensory and motor function (areas 40, 43, and 44 at inferior pericentric gyri), and, particularly, language and speech (areas 44, 45, posterior part of area 22, and area 39) (Fig 1).

Anatomically, the cerebral operculum is on the lateral convexity of the hemisphere, composed of the inferior frontal gyrus anterosuperiorly (the frontal operculum), the inferior pericentric gyri superiorly, the supramarginal and angular gyri superoposteriorly (the parietal operculum), and the superior temporal gyrus inferiorly (the temporal operculum). The inferior frontal gyrus is divided by anterior ascending and horizontal rami of the sylvian fissure into three parts: (1) pars orbitalis, (2) pars triangularis, and (3) pars opercularis (1). The pars triangularis and opercularis in the dominant hemisphere are referred to as "Broca's area" (concerned with motor aspects of speech). The inferior precentral, central, and postcentral sulci separate the parietal operculum into precentral, postcentral, and supramarginal gyri. The supramarginal gyrus forms a horseshoe gyrus draped over the superior end of the posterior ramus of the sylvian fissure. The angular gyrus similarly forms a horseshoe gyrus hooking around the posterior end of the superior temporal sulcus. The superior temporal gyrus inclines posterosuperiorly to fuse with the supramarginal and angular gyri. The superior temporal sulcus runs parallel to the superior temporal gyrus and separates it from the middle temporal gyrus. The opercular surface anatomy features bear fairly constant relationships, making multiplanar MR evaluation feasible (3, 4).

Embryologically, opercularization (the development of the operculum) begins by 20 to 22 weeks, starting after the cortical plate becomes

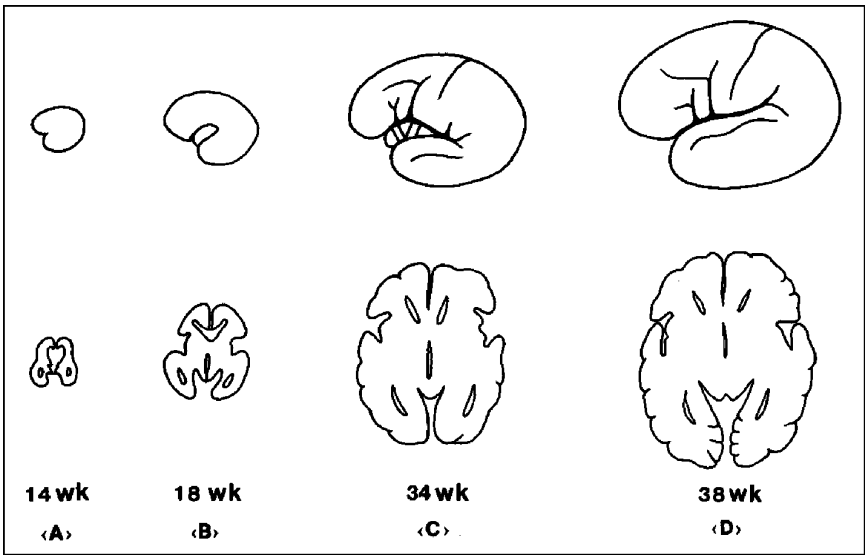

Fig 7. Schematic illustration of the normal opercularization at 14, 18, 34, and 38 weeks of gestation from lateral views of fetal hemisphere and on axial planes at the level of the hypothalamus.

focally thickened and indented at the insular region around the 20th week of gestation. The bulky outgrowth of the posterior operculum (the temporal and parietal lobes) develops faster than the anterior operculum (the frontal lobe), eventually folding over to engulf the insular area, forming the posterior (horizontal) sylvian fissure. The anterior part of the insula remains exposed almost until the frontal lobe overrides the insula at the term of gestation (6, 12) (Fig 7). Thus, the process of opercularization is from posterior to anterior and should be completed by birth. Therefore, the opening of any part of the operculum with an insula that is exposed might indicate a delay in reaching developmental milestones.

Location of the surface anatomy of the brain has been studied since the advent of computed tomography (CT) with axial planes (11, 13), and then later, with MR, mainly in the sagittal plane (3–5). Certain gyri or sulci that can be topographically identified are based on tracing or by deducing from the known major surface landmarks, ones that are relatively constant in appearance on imaging planes. Kido et al used the superior frontal sulci as a guide to identify the precentral and central sulci at the high convexity of the hemisphere on axial CT (11). They concluded that the inferior parts of these gyri and sulci also could be traced. In our study, we used the circular sulcus (the perinsular sulcus) more often than the superior frontal sulcus as a guide to locate the inferior precentral sulcus and the anterior ascending ramus of the sylvian fissure, which are important landmarks for identification of Broca's area in the dominant hemisphere with axial MR images. We often had trouble tracing the precentral sulcus from the high convexity inferiorly, because with some cases there is a gap in the precentral sulcus at the point where the middle frontal gyrus fuses with the precentral gyrus. The anterior border of the circular sulcus can be confidently identified in every case, and this is the point where the anterior ascending ramus of the sylvian fissure starts. The inferior precentral, central, and postcentral gyri are the next three sulci anterior to the ascending ramus of the sylvian fissure. As shown in "Results," we could locate the inferior precentral sulcus on axial MR images in 94.4% of cases. We believe the same technique can be applied to axial CT. Another useful guide used in this study for identification of the supramarginal and angular gyri is the interparietal sulcus. This sulcus runs in anteroposterior direction to separate the parietal lobe into medial and lateral halves. It fuses with the postcentral sulcus in most instances and, therefore, serves to locate the supramarginal gyrus, which is posterior to the postcentral sulcus and lateral to the interparietal sulcus. The angular gyrus, which is important for perception of written language, is located posterior to the supramarginal gyrus and lateral to the interparietal sulcus.

Sagittal MR remains the most useful imaging plane in topographic identification of the opercular surface anatomy, as shown in our study and in those of others (3, 4). Again, the anterior

border of the circular sulcus serves as the best guide to find the anterior ascending ramus of the sylvian fissure in the continuous sections. Other important areas, such as the supramarginal and angular gyri, as well as the superior temporal gyrus, can be directly located without difficulty. Coronal MR images also can be used to identify important opercular anatomy, including the inferior frontal gyrus, inferior precentral gyrus, superior temporal gyrus, supramarginal gyrus, and, to a lesser extent, the angular gyrus. The disadvantages of the coronal plane are that some major sulci (ie, the precentral and central sulci), which run parallel to the imaging planes, cannot be identified with certainty. Our study indicated that by using axial, coronal, and sagittal MR imaging, most of the important surface anatomy of the operculum can be identified. In some cases, even when sagittal planes are not available, the axial with coronal MR images help in location of the opercular structures.

As described previously, the sylvian fissure is where the opercula appose. Thus, the width of the sylvian fissure may be associated, to some degree, with opercular development. Tatum et al used axial T1-weighted images to measure the normal frontotemporal separation in 125 pediatric scans and concluded that the normal separation of the sylvian fissure should not exceed 3 mm. They made further comments that the wide sylvian fissure (the open operculum sign) may represent developmental arrest and is probably a marker of more diffuse brain abnormalities (7). In our study, not only the frontotemporal separation (the anterior sylvian width or anterior interopercular distance in this article) but also the parietotemporal separation (the posterior sylvian width or posterior interopercular distance) were measured in more imaging planes. Although our measurement results were obtained from two groups with two different age ranges (from newborn to 1 year and 1 year and older), not specifically age matched by month, it may, like the other normal measurement studies, provide the radiologist and even the clinician a guideline concerning the normal MR anatomy and sylvian width in different section planes. Infants or children with more than normal sylvian fissure width in an otherwise normal cerebral MR images may be healthy or associated with clinical developmental delay (particularly the language development). On the contrary, we have seen many patients with significant clinical delay, neurologic deficit, or craniofacial anomaly showing wide interopercular distance (open operculum).

The results of our study reflects the fact that the embryologic process of opercularization starts from the posterior to the anterior. The posterior interopercular distance was small ($<$1.8 mm) in healthy infants and continued to decrease in childhood ($<$0.5 mm). The anterior interopercular distance was significantly wider than its posterior counterpart, both in infants ($<$4.5 mm) and in children ($<$3.5 mm). The consistent smaller posterior interopercular distance and wider anterior interopercular distance are apparently attributable to rapid enlargement of the posterior temporal and parietal operculum, which result in tightness of the posterior operculum during the development of the cerebral hemisphere within the calvarium. Other interesting findings in our study were the left-right asymmetry of the anterior interopercular distances in infants. The left anterior interopercular distance was significantly larger than the right ($P < .05$). Embryologically, it would appear that the right hemisphere develops its sulci and fissures earlier than the left, and that the left hemisphere is usually larger than the right because of hemispheric dominance (14). Our results coincided with that of Seidenwurm et al, who used axial CT to measure the size of the sylvian fissure in 32 infants (15).

In conclusion, the operculum should be evaluated with MR in three planes. Infants may show conspicuous sylvian fissures that should not exceed 4.5 mm (mean + 2 SD) anteriorly on axial and sagittal planes and 1.8 mm posteriorly on sagittal and coronal planes. Healthy children who have fully developed opercula should have an anterior interopercular distance of no more than 3.5 mm and a posterior interopercular distance of 0.5 mm. MR appears to be the modality of choice in identification of the opercular surface anatomy and quantitative evaluation of the normal opercularization of the brain.

Acknowledgments

We thank Valerie Tsafos and Rachel Zimmerman for their assistance in manuscript preparation and photography.

References

1. Carpenter MB. *Core Text of Neuroanatomy*. 4th ed. Baltimore, Md: Williams & Wilkins; 1991:133–156
2. deGroot J, Chusid JG. *Correlative Neuroanatomy*. 12th ed. Prentice-Hall International Inc; 1988:189–196
3. Ebeling U, Steinmetz H, Huang Y, Kahn T. Topographic identification of the inferior precentral sulcus in MR imaging. *AJNR Am J Neuroradiol* 1989;10:937–942
4. Steinmetz H, Ebeling U, Huang Y, Kahn T. Sulcus topography of the parietal opercular region: an anatomic and MR study. *Brain Lang* 1990;38(4):515–533
5. Naidich TP. MR imaging of brain surface anatomy. *Neuroradiology* 1991;33(suppl):s95–s99
6. Larroche JCL. Development of the central nervous system. In: *Developmental Pathology of the Neonate*. Amsterdam: Excerpta Medica; 1977:319–327
7. Tatum WO, Coker SB, Ghobrial M, Shamel A-A. The open opercular sign: diagnosis and significance. *Ann Neurol* 1989;25:196–199
8. Brodmann K. *Vergleichende Lokalisationlehre der Grosshirnrinde in ihren Prinzpien dargestelt auf Grund des Zellenbaues*. Leipzig, Germany: JA Barth; 1990:324
9. Martin E, Kikinis R, Zuerrer M, et al. Developmental stages of human brain: an MR study. *J Comput Assist Tomogr* 1988;12(6):917–922
10. Functional neuroanatomy of man. In: Williams PL, Warwick R, eds. *Gray's Anatomy*. Edinburgh: Churchill Livingstone, 1975
11. Kido DK, LeMay M, Levinson AW, Benson WE, RT. Computed tomographic localization of the precentral gyrus. *Radiology* 1980;135:373–377
12. Moore KL. *The Developing Human*. 5th ed. Philadelphia, Pa: WB Saunders Co; 1993:385–422
13. Ebeling U, Huber P, Reulen HJ. Localization of the precentral gyrus in the computed tomogram and its clinical application. *J Neurol* 1986;233:73–76
14. Geschwind N, Livitsky W. Human brain: left-right asymmetries in temporal speech regions. *Science* 1968;161:186–187
15. Seidenwurm D, Bird CR, Enzmann DR, Marshall WH. Left-right temporal region asymmetry in infants and children. *AJNR Am J Neuroradiol* 1985;6(5):777–779